PCCP

Accepted Manuscript

ROYAL SOCIETY OF CHEMISTRY

www.rsc.org/pccp

PCCP

RSCPublishing

COMMUNICATION

Selectively splitting a droplet using superhydrophobic stripes on hydrophilic surfaces†

Dong Song,[a] Baowei Song,[a]* Haibao Hu,[a] * Xiaosong Du, [b]* and Feng Zhou[c]

Superhydrophobic patterns were fabricated on hydrophilic surfaces by selective painting. The impinging process of water droplets on these hybrid surfaces was investigated. The droplet can be split by impinging on the hydrophilic surface with a single stripe at a high velocity. The time to split the droplet is independent of the impact velocity and it is smaller than the contact time of a droplet impinging on the fully superhydrophobic surface. The volume ratios of the split mini-droplets could be precisely controlled by adjusting the landing position of the original droplet. The droplet could be split uniformly into more mini-marbles by increasing the stripe numbers.

Superhydrophobic surfaces are the surfaces with high contact angle and low contact angle hysteresis where the water droplets can roll off easily as seen in Figure 1a. It has received extensive attention in the past decades with applications in many fields, e.g. drag reduction[1, 2], self-cleaning[3], heat transfer enhancement[4], anti-icing[5], etc. While on the hydrophilic surfaces, as seen in Figure 1b, the contact angle is small and the droplets would stick on the surfaces even at a large tilted angle. The combination of superhydrophobicity and hydrophilicity on one surface gives rise to some exciting properties and potential engineering applications, e.g. patterning complex geometries with liquids[6, 7], biomolecular manipulation at surface/interface[8-11], offset printing[12], open-air microfluidic device[13-15], droplet manipulation[16, 17] and so on. By modifying the wetting characteristics of surfaces, we can move, deflect and sort droplets[18] or transport fluid without power input[19]. Using superhydrophobic blades, a droplet can be cut without formation of tiny satellite droplets[20-22]. To the best of knowledge, previous work has been focused on the fabrication techniques and characterization of the static wettability on these hybrid surfaces[6]. In this communication, we report a new application of these surfaces to split an impinging droplet by coated superhydrophobic stripes on a hydrophilic surface. These results provide insights into a route for miniaturized patterning/split of liquids and have a potential for manipulation of droplets in microfluidics and biomedical applications[23].

Superhydrophobic patterns were fabricated on a hydrophilic glass slide using a commercial coating, Ultra-Ever Dry (Ultra Tech International Inc). The substrate was patterned by shadow mask[24] during the spray coating (air pressure ~ 0.5MPa). The sample was annealed in an oven at 60℃ for 10 minutes. Thickness of the coating (~ 50μm) was determined by profilometry. The impact process of droplets on the hybrid surfaces was captured using a high speed camera (MotionXtra NX-4, IDT Corporation) with 5000 fps at a resolution of 600×600 pixels. The droplets were released from a stainless steel needle right above the surface. The diameter of the droplet is 3.1±0.2 mm. The impinging velocity was adjusted by varying the height of the needle from the surface. The landing position of the droplet on the surfaces was estimated from the image sequence. Each of the impact experiments were conducted at least 3 times.

The coated surface is superhydrophobic with a contact angle about 165° and a contact angle hysteresis within 2° (Figure 1a). The glass substrate is hydrophilic with a contact angle around 50° and a contact angle hysteresis 75° (Figure 1b). An instant picture of a droplet impinging on the hybrid surface is shown in Figure 1c. On the hydrophilic area the surface tension of the solid surface at the three-phase contact line, $\gamma_{sg} - \gamma_{sl} = \gamma \cdot \cos\theta_{phi}$, stretches the droplet outward thereby hindering the retraction of the three-phase contact line. Here γ_{sg}, γ_{sl}, γ, θ_{phi} are the surface tension of solid-gas, solid-liquid, liquid-gas and the contact angle on the hydrophilic surface, respectively. However on the superhydrophobic stripe, the surface tension of the solid surface at the three-phase contact line, $\gamma_{sg} - \gamma_{sl} = \gamma \cdot \cos\theta_{pho}$, pulls the droplet inward along the direction parallel to the stripe inducing the three-phase contact line to retract fast, where θ_{pho} is the contact angle on the superhydrophobic surface. This unbalanced surface tension along the three-phase contact line enables the superhydrophobic stripe to act like a blade and split the droplet into halves eventually.

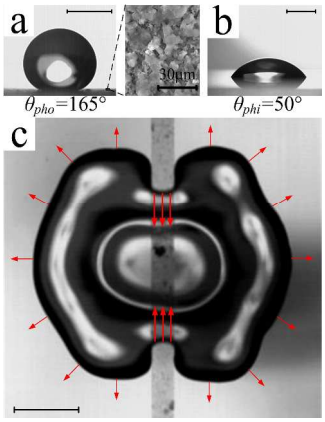

Figure 1. Droplets on: (a) the superhydrophobic surface coated by Ultra-Ever Dry and (b) the hydrophilic glass slide. (c) The droplet impinging on the hydrophilic surface coated with a narrow superhydrophobic stripe (gray area). The impact velocity is 0.97m/s. Scale bar 2mm.

To gain more insights from the impact process on these surfaces, we investigated the details using a high speed camera. When a droplet impinged on a hydrophilic surface, as shown in Figure 2a (Video_Fig_2a.mpg in the Supporting Information), it would spread quickly to the maximum diameter and then recoils very slowly. The hydrophilic surface has a high surface energy in air and a low interfacial energy with water. This property enables the hydrophilic surface to absorb most of the kinetic energy of the droplet, leading to the droplet sticking onto the hydrophilic surface. However, the superhydrophobic surface behaves oppositely where the air trapped within the micro-structures even decreases the absorption of the kinetic energy. This gave rise to the droplet rebounce from the superhydrophobic surface (see Figure 2b and Video_Fig_2b.mpg in the Supporting Information). It is interesting to note that a vertical satellite jet formed on the top of the droplet at 18 ms. When a droplet impinged on the hydrophilic surface with a superhydrophobic stripe, as seen in Figure 2c (side view) and d (top view) (Video_Fig_2c.mpg and Video_Fig_2d.mpg in the Supporting Information), the maximum spreading diameter in the direction parallel to the stripe was greatly reduced, whereas the fluid retracted so fast on the superhydrophobic stripe that the droplet was split into halves in the end.

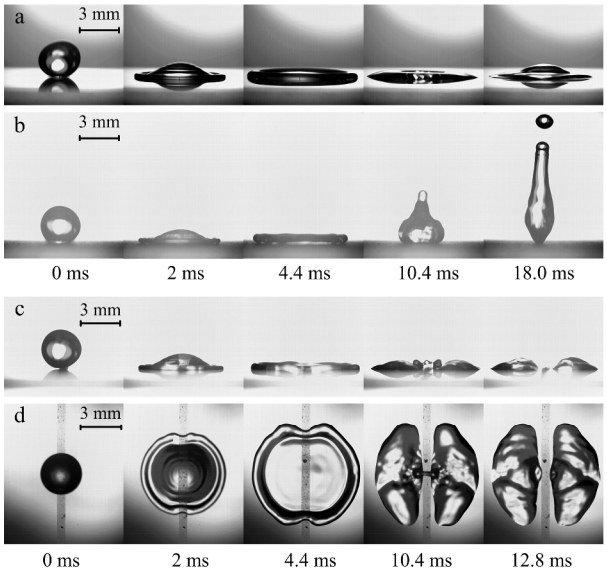

Figure 2. Impinging processes of droplets on (a) the hydrophilic glass surface, (b) the superhydrophobic surface, (c) and (d) the hydrophilic surface with one superhydrophobic stripe. The diameter of the droplet is 3.1 mm and the impact velocity is 0.97 m/s.

The dynamic diameter of the droplet and length of the fluid on the superhydrophobic stripe area during the impact process is shown in Figure 3. The value is normalized by the droplet diameter (D_0=3.1 mm). The weber number is in the terms of $We = \rho U^2 D_0/\gamma$, where ρ, U are the water density and imping velocity, respectively. On the hydrophilic surface (filled squares in Figure 3), the droplet failed to recoil after spreading to the maximum diameter which is much larger than that on other surfaces. On the superhydrophobic surface (filled circles in Figure 3), the droplet retracts very fast after spreading to its maximum diameter leading to the total contact time within 18 ms. On the hydrophilic surface with one hydrophobic stripe (hollow squares in Figure 3), the maximum diameter on the stripe is close to that on the fully coated superhydrophobic surface when the impinging velocity is the same. Surprisingly, the retraction velocity at the superhydrophobic stripe area is larger than that on the fully superhydrophobic surface corresponding to a splitting time around 12.2 ms. If we assume the droplet is a uniform flattened sheet with thickness h, the droplet would retract uniformly with the recoiling velocity as $V_r = \sqrt{2\gamma/(\rho h)}$ [25]. If the thickness is not uniform, the droplet would retract faster in the thinner region where there is less mass to accelerate. Bird *et. al*[5] succeeded in reducing the contact time of a droplet by introducing a thin rib on the superhydrophobic surface. The reduced contact time can be estimated as $\Delta T = \frac{\sqrt{6}}{6}(1-\sqrt{1-a/h})\cdot\tau$, where a is the thickness of the rib, and $\tau = (\rho R_0^3/\gamma)^{1/2}$ is the inertial-capillary timescale and R_0 is the droplet radius. Because the thickness of our superhydrophobic coating is around 50μm, the reduced thickness of the droplet sheet on the coated stripe results in the faster retraction process and the smaller splitting time than those on the fully superhydrophobic surface. At a high impact velocity (the blue symbols and the inset a in Figure 3), corresponding to $We \geq 20$, the droplet can be split with the splitting time irrespective of impinging velocities. This observation is consistent with previous study that the droplet contact time T is independent of the impact velocity[26]. Once the impact velocity is smaller than a critical value, i.e. $We < 20$ (the green symbols and the inset b in Figure 3), the droplet will remain intact upon impinging.

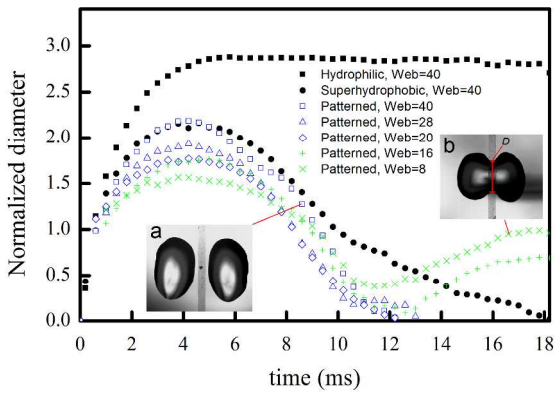

Figure 3. The dynamic diameter of the contact area changes as a function of time. The value is normalized by droplet diameter (D_0 = 3.1 mm). (■) and (●) represent the three-phase contact line diameters on the hydrophilic surface and the superhydrophobic surface, respectively. The blue and green symbols correspond to the length of the fluid on the stripe area as marked in inset b. Blue symbols (□ △ ◇) represent large weber numbers when the droplets were successfully split (as seen in the inset a). Green symbols (+ ×) represent smaller weber numbers when the droplets failed to be split (as seen in the inset b).

The volume ratios of the split droplets can be controlled by adjusting the droplet landing position. Figure 4 shows the volume fractions of the split droplets as a function of the landing point moving from the center of the stripe to the right side of hydrophilic substrate. The volume fractions were normalized in term of: V/V_0, where V_0 is the volume of the original droplet. It is interesting to note that the volume ratio of the split droplets is in good agreement with the area ratio of the flattened droplet on two sides of the stripe at its maximum diameter.

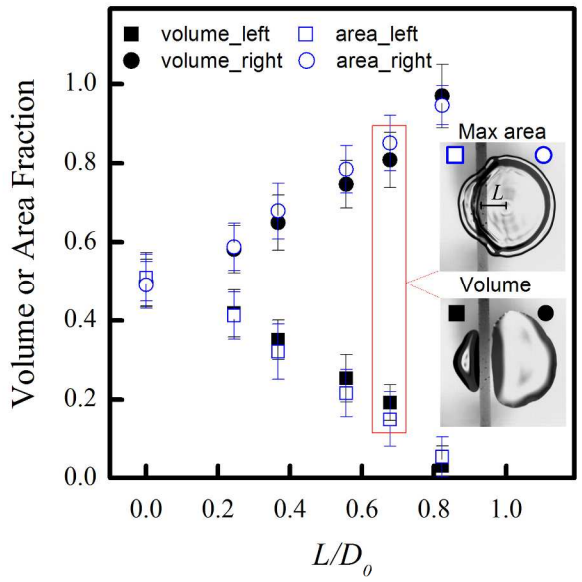

Figure 4. Volume and area fractions of the split droplets on two sides of the stripe as the landing position moves from center to the right side of the stripe (L/D_0 increasing). (■,●) represent the volume fractions of the split droplets and (□,○) represent the area fractions of the flattened droplet on two sides of the stripe when the droplet spreads to the maximum area. The insets show the instant images of the split droplets by the stripe and the flattened droplet at the maximum area. L is the distance between the landing point and the center line of the stripe. We = 40 in these experiments.

The droplet can be split into more mini-marbles by using more stripes. Figure 5(a, b, c) shows the results of a droplet impinging on a hydrophilic surface with two superhydrophobic stripes crossing each other. By varying the landing position, the droplet can be split into four satellite droplets with controllable volume ratios. As shown in Figure 5(a, d, e, f), the droplet can be uniformly split into multiple mini-marbles (n = 2, 3, 4 and 6) by landing the droplet on the center of the coated hydrophobic pattern.

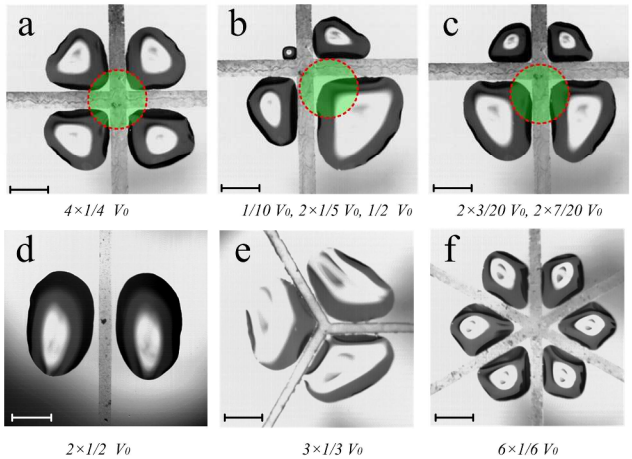

Figure 5. Droplets split into mini-marbles using a series of superhydrophobic stripes. (a-c) The droplets were split into four parts with controllable volume fractions by adjusting the landing position. The green shadows circled by red dots show the size and landing position of the droplet. (d-f) The droplets were uniformly split into multiple mini-marbles. Scale bar 2 mm.

In summary, we reported a new method to split a droplet by introducing narrow superhydrophobic stripes on a hydrophilic surface. The unbalanced surface tension at the superhydrophobic/hydrophilic interface led to different retraction velocities and the final split of the droplet. The time to split the droplet by the superhydrophobic stripe is smaller than the contact time on the fully superhydrophobic surface, regardless of the impinging velocity. The droplet will not be split by the stripe if the impinging velocity is smaller than a critical value. By adjusting the droplet landing position, the droplet could be split into mini-droplets with controllable ratios. The droplet can be uniformly split into multiple mini-marbles by increasing the number of stripes.

This research was supported by National Nature Science Foundation of China (No. 51109178), Science and Technology Innovation Foundation of NWPU (JC20120218), and the Doctorate Foundation of Northwestern Polytechnical University(CX201206). Xiaosong Du acknowledges funding support from the Juvenile Diabetes Research Foundation (3-PDF-2014-113-A-N).

Notes and references

[a] School of Marine Science and Technology, Northwestern Polytechnical University, 127 Youyi Xilu, Xi'an, 710072, Shaanxi, P. R. China.
*Email: songbaowei@nwpu.edu.cn (Baowei Song), huhaibao@nwpu.edu.cn (Haibao Hu);
[b] Microproducts Breakthrough Institute, Corvallis, Oregon, 97330, USA.
*Email: dxs571@vt.edu (Xiaosong Du).
[c] State Key Laboratory of Solid Lubrication, Lanzhou Institute of Chemical Physics, Chinese Academy of Sciences, Lanzhou 730000, PR China.
† Electronic Supplementary Information (ESI) available: The videos associated with the droplet impinging processes shown in Figure 2.

1. J. Ou and J. P. Rothstein, *Physics of Fluids*, 2005, **17**, 103606.
2. J. P. Rothstein, *Annu Rev Fluid Mech*, 2010, **42**, 89-109.
3. M. Yu, S. Chen, B. Zhang, D. L. Qiu and S. X. Cui, *Langmuir*, 2014, **30**, 13615-13621.
4. N. Miljkovic, R. Enright and E. N. Wang, *Acs Nano*, 2012, **6**, 1776-1785.
5. J. C. Bird, R. Dhiman, H. M. Kwon and K. K. Varanasi, *Nature*, 2013, **503**, 385-388.
6. E. Ueda and P. A. Levkin, *Adv Mater*, 2013, **25**, 1234-1247.
7. M. J. Hancock, F. Yanagawa, Y. H. Jang, J. K. He, N. N. Kachouie, H. Kaji and A. Khademhosseini, *Small*, 2012, **8**, 393-403.
8. A. L. Hook, N. H. Voelcker and H. Thissen, *Acta Biomater*, 2009, **5**, 2350-2370.
9. L. Yuan, Q. Yu, D. Li and H. Chen, *Macromol Biosci*, 2011, **11**, 1031-1040.
10. J. D. Kittle, X. Du, F. Jiang, C. Qian, T. Heinze, M. Roman and A. R. Esker, *Biomacromolecules*, 2011, **12**, 2881-2887.
11. A. Kaya, X. Du, Z. Liu, J. W. Lu, J. R. Morris, W. G. Glasser, T. Heinze and A. R. Esker, *Biomacromolecules*, 2009, **10**, 2451-2459.
12. S. Nishimoto, A. Kubo, K. Nohara, X. Zhang, N. Taneichi, T. Okui, Z. Liu, K. Nakata, H. Sakai, T. Murakami, M. Abe, T. Komine and A. Fujishima, *Appl Surf Sci*, 2009, **255**, 6221-6225.
13. M. Elsharkawy, T. M. Schutzius and C. M. Megaridis, *Lab Chip*, 2014, **14**, 1168-1175.
14. C. J. Huang, W. F. Fang, M. S. Ke, H. Y. E. Chou and J. T. Yang, *Lab Chip*, 2014, **14**, 2057-2062.
15. X. Du, C. J. Durgan, D. J. Matthews, J. R. Motley, X. Tan, K. Pholsena, L. Árnadóttir, J. R. Castle, P. G. Jacobs, R. S. Cargill, W. K. Ward, J. F. Conley and G. S. Herman, *ECS Journal of Solid State Science and Technology*, 2015, **4**, P3069-P3074.
16. S. Varagnolo, V. Schiocchet, D. Ferraro, M. Pierno, G. Mistura, M. Sbragaglia, A. Gupta and G. Amati, *Langmuir*, 2014, **30**, 2401-2409.
17. A. Dupuis, J. Leopoldes, D. G. Bucknall and J. M. Yeomans, *Appl Phys Lett*, 2005, **87**.

18. M. A. Nilsson and J. P. Rothstein, *Phys Fluids*, 2012, **24**, 062001 .
19. A. Ghosh, R. Ganguly, T. M. Schutzius and C. M. Megaridis, *Lab Chip*, 2014, **14**, 1538-1550.
20. E. Bormashenko and Y. Bormashenko, *Langmuir*, 2011, **27**, 3266-3270.
21. R. Yanashima, A. A. Garcia, J. Aldridge, N. Weiss, M. A. Hayes and J. H. Andrews, *Plos One*, 2012, **7**, e45893.
22. H. Mertaniemi, V. Jokinen, L. Sainiemi, S. Franssila, A. Marmur, O. Ikkala and R. H. A. Ras, *Adv Mater*, 2011, **23**, 2911-2914.
23. S. H. Ma, J. M. Sherwood, W. T. S. Huck and S. Balabani, *Lab Chip*, 2014, **14**, 3611-3620.
24. X. Du, B. T. Flynn, J. R. Motley, W. F. Stickle, H. Bluhm and G. S. Herman, *ECS Journal of Solid State Science and Technology*, 2014, **3**, Q3045-Q3049.
25. F. E. C. Culick, *J Appl Phys*, 1960, **31**, 1128-1129.
26. D. Richard, C. Clanet and D. Quere, *Nature*, 2002, **417**, 811-811.

